Hindawi
Mathematical Problems in Engineering
Volume 2018, Article ID 2179617, 7 pages
https://doi.org/10.1155/2018/2179617

Research Article

A Spectrum Efficient Secure Transmission Scheme Based on Directional Polarization Modulation for Wireless Communication Systems

Zhongmin Pei, Zhangkai Luo, and Bo Zou

Science and Technology on Complex Electronic System Simulation Laboratory, Space Engineering University, Beijing 101400, China

Correspondence should be addressed to Zhangkai Luo; 1440118915@qq.com

Received 15 October 2018; Accepted 11 November 2018; Published 26 November 2018

Academic Editor: Francesca Vipiana

In this paper, a spectrum efficient secure transmission scheme based on directional polarization modulation (DPM) is proposed. Specifically, the polarized signals are divided into two parts, i.e., I and Q, and a dual-polarized antenna array is designed to form beams to transmit these signals. Naturally, the constellation structure is associated with the beam gain, which can be controlled to make the constellation structure distort in undesired directions. Thus the security is enhanced for the symbol error rate performance deteriorates in undesired directions. Additionally, a kind of directional modulation technique is utilized to transform one component of the polarized signal into QPSK signal and thus improves the modulation order without extra transmitting power consummation. Finally, theoretical analysis and simulation results demonstrate that the proposed scheme can improve the transmission efficiency and provide a security transmission method for wireless communication systems.

1. Introduction

In order to meet the ever increasing high data rate demand, the fifth generation (5G) of wireless cellular communication systems is predicted to be available to the market by 2020 [1, 2]. To alleviate the scarcity of spectrum resources, 5G is suggested to be working in millimeter-wave (mm-wave) bands. However, in the mm-wave communication, the non-line-of-sight (NLOS) signals are very weak due to the large path loss. Thus, multiple-input multiple-output (MIMO) techniques are hard to be applied to improve the transmission efficiency, for MIMO gains depend on the decorrelation between channels [3]. Fortunately, polarization diversity is proved to be a feasible way to improve the transmission efficiency for it can provide two independent paths on the same frequency band in line-of-sight (LOS) channels [4, 5]. Furthermore, in addition to the traditional polarization diversity and polarization multiplexing, the polarization state is explored to carry information and the technology is called polarization modulation (PM), which can be combined with traditional modulation techniques without contradictions [6] and improve the energy efficiency [7].

On the other hand, the transmit information is easy to be eavesdropped due to the openness nature of the wireless medium [8]. The information security is important and receives more and more attention in recently years. Transmission security is traditionally dependent on cryptographic techniques in the link and network layer. Challenges (and vulnerabilities) associated with key distribution and management, however, make cryptography a less than ideal solution [9]. Fortunately, new research on physical layer security brings new ways with great potential, which focus on preventing eavesdroppers from decoding any useful message intended to the desired user.

In the traditional mode, modulated radio frequency (RF) signals go through a power amplifier to drive the transmit antenna or antenna array. It is noteworthy that there is a great possibility for a sufficiently sensitive eavesdropper to recover information from the signal that is transmitted through side lobes, whose only difference from the signal received in the main lobe is the signal's power. To address this problem, in [10, 11], directional modulation (DM) is proposed, in which the transmit signal is direction-dependent and the signal can be purposely distorted in undesired directions. In [12], a

dual-beam DM technique is introduced, which utilizes dual beams to form a secure link from the transmitter to the receiver. In [13–15], multipath directional modulation is proposed to provide multisecure links to receivers. However, the above researches are based on the scalar array and little literature reports the DM with the dual-polarized array.

Motivated by the above, we propose a spectrum efficient directional polarization modulation (SEDPM) scheme in this paper, which can improve the transmission efficiency and security at the same time. In the SEDPM scheme, two components of the polarized signal are both divided into two data streams and transmitted by four orthogonal beams formed by the dual-polarized antenna array. In this way, the transmit signals' constellation structure is associated with the array gain and only in the desired direction that the constellation structure is not distorted. Therefore, the security is enhanced due to the symbol error rate (SER) increases in undesired direction. Additionally, to maximize the spectrum efficiency, the component of the polarized signal that contains only the real number is transformed into the QPSK signal [12] and this kind of transformation has no influence on the demodulation of the PM signal; thus two kinds of modulation technique can be combined and the spectrum efficiency is improved.

In this letter, we assume an AWGN channel, infinite XPD, and evaluate the achievable security performance of the proposed scheme. Although nonideal XPD is an important consideration for the proposed scheme, its effect is less in the Ku band and precompensation methods [17, 18] can also reduce the influence. In addition, we assume the equal transmission path length between two polarization channels and there is no frequency offset for these problems are solved in [19].

2. Signal Model

The electromagnetic wave emitted from the antenna is $s_0 = Ae^{(j(w_c t+\phi))}$ [20], where A denotes the amplitude, w_c denotes the carry frequency, and ϕ denotes the initial phase, which is set to 0 for simplifying the analysis. Two components of the polarized signal can be denoted as

$$\mathbf{s}(t) = \begin{bmatrix} s_1 \\ s_2 \end{bmatrix} = \begin{bmatrix} \cos\gamma \\ \sin\gamma e^{j\eta} \end{bmatrix} s_0, \tag{1}$$

where $\gamma \in [0, \pi/2], \eta \in [0, 2\pi]$ are polarization parameters. s_1 and s_2 denote the two components, respectively.

Indeed, the polarized signal's polarization state (PS) is determined by (γ, η), and M_1-th order constellation points can be represented as $PS_k : (\gamma_k, \eta_k), k = 1, 2, \cdots, M_1$. For the k-th constellation point, we take the real part of (1) and derive the real modulated signal as

$$\begin{aligned} \mathrm{Re}[s(t)] &= \mathrm{Re}\left[A \begin{bmatrix} \cos\gamma_k e^{jw_c t} \\ \sin\gamma_k e^{j\eta_k} e^{jw_c t} \end{bmatrix} \right] \\ &= A \begin{bmatrix} \cos\gamma_k \cos w_c t + 0 * \sin w_c t \\ \sin\gamma_k \cos\eta_k \cos w_c t - \sin\gamma_k \sin\eta_k \sin w_c t \end{bmatrix}. \end{aligned} \tag{2}$$

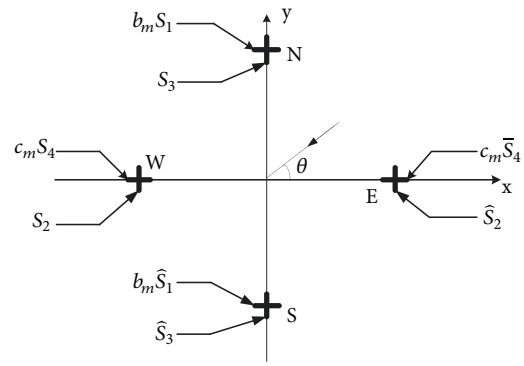

Figure 1: Signal transmission design.

As we can see, two components of the polarized signal are both divided into I and Q parts, which will be separately transmitted in the SEDPM scheme.

3. Principle of the SEDPM Scheme

3.1. Signal Transmission. We consider a dual-polarized antenna array as shown in Figure 1 in the x−y coordinate system; N, W, E, and S are used to mark the four elements. N_1 and N_2 are two orthogonal polarized components of the dual-polarized antenna N, where N_1 is parallel to the x axis and N_2 is vertical to the x axis. In addition, the same is to W_1, W_2, E_1, E_2, S_1, and S_2. According to [12], inverse-excitations are taken to drive the copolarization antennas N_1 and S_1 (N_2 and S_2), then the radiation pattern can be expressed as

$$f_1(\theta) = \sin\left(\frac{\pi d}{\lambda} \cos(\theta) \right), \tag{3}$$

where λ denotes the wavelength, θ denotes the azimuth angle and $d = \lambda/2$ denotes the distance between antenna elements in the same axis. Similarly, the radiation pattern of W − E can be written as

$$f_2(\theta) = \sin\left(\frac{\pi d}{\lambda} \sin(\theta) \right). \tag{4}$$

The beam pattern of $f_1(\theta)$, $f_2(\theta)$ and the normalized synthesized pattern $f(\theta) = \sqrt{f_1^2(\theta) + f_2^2(\theta)}$ are shown in Figure 2.

In order to improve the spectrum efficiency and security performance, we replace the $\cos\gamma_k \cos w_c t$ in (5) by

$$\frac{\cos\gamma_k b_m}{\sqrt{2}} \cos w_c t + \frac{c_m \cos\gamma_k}{\sqrt{2}} \sin w_c t, \tag{5}$$

where $b_m \in \{-1, 1\}$ and $c_m \in \{-1, 1\}$. By selecting different values of b_m and c_m, we can realize QPSK in polarization 1 like the manner in [12]. In addition, both two components of the polarized signal are divided into two parts, which will be transmitted by designed beams separately. The excitation signals for each antenna are shown in Table 1, where $\widehat{S}_1, \widehat{S}_2, \widehat{S}_3, \widehat{S}_4$ are phase inverse ones of S_1, S_2, S_3, S_4 and $S_1 = (\cos\gamma_k/\sqrt{2}) \cos w_c t$ $S_2 = \sin\gamma_k \cos\eta_k \cos w_c t$, $S_3 = -\sin\gamma_k \sin\eta_k \sin w_c t$, and $S_4 = (\cos\gamma_k/\sqrt{2}) \sin w_c t$ [12].

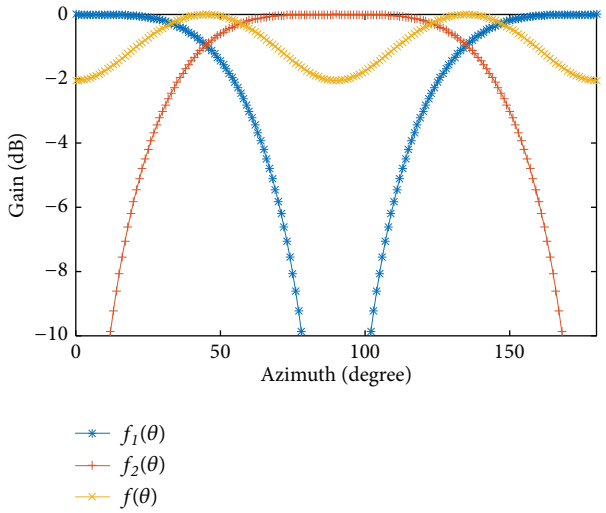

Figure 2: Beam gain of the dual-polarized array.

Table 1: Excitation signals of each antenna.

Antenna Polarization 1	excitation signal	Antenna Polarization 2	excitation signal
N_1	$b_m S_1$	N_2	S_3
W_1	$c_m S_4$	W_2	S_2
S_1	$b_m \widehat{S}_1$	S_2	$\widehat{S}_3$
E_1	$c_m \widehat{S}_4$	E_2	$\widehat{S}_2$

3.2. Signal Demodulation. At the receiver side, the signal demodulation can be divided into two steps: the demodulation of the QPSK signal in polarization 1 and the demodulation of PM signal. We assume that there is no depolarization effect; then, the received signal can be expressed as

$$\begin{aligned}\mathbf{y} &= \begin{bmatrix} F_1 \\ F_2 \end{bmatrix} \\ &= A \begin{bmatrix} \dfrac{\left(f_1(\theta) b_m \cos\gamma_k \cos w_c t + f_2(\theta) c_m \cos\gamma_k \sin w_c t\right)}{\sqrt{2}} + n_1 \\ \sin\gamma_k \begin{pmatrix} f_1(\theta)\cos\eta_k \cos w_c t \\ -f_2(\theta)\sin\eta_k \sin w_c t \end{pmatrix} + n_2 \end{bmatrix} \\ &= A \begin{bmatrix} \dfrac{f(\theta)\cos\gamma_k \cos\left(w_c t - \varphi_1\right)}{\sqrt{2}} + n_1 \\ \widehat{f}(\theta)\sin\gamma_k \cos\left(w_c t + \varphi_2\right) + n_2 \end{bmatrix} \end{aligned} \tag{6}$$

where

$$\begin{aligned} f(\theta) &= \sqrt{f_1^2(\theta) + f_2^2(\theta)} \\ \widehat{f}(\theta) &= \sqrt{\left(f_1(\theta)\cos\eta_k\right)^2 + \left(f_2(\theta)\sin\eta_k\right)^2}, \end{aligned} \tag{7}$$

and $\varphi_2 = \arctan((f_2(\theta)/f_1(\theta))\tan\eta_k)$ and $\varphi_1 = \arctan(c_m f_2(\theta)/b_m f_1(\theta))$.

Table 2: QPSK modulation in polarization 1.

b_m	c_m	QPSK in polarization 1
1	1	$f(\theta)\cos\gamma_k \angle \dfrac{f_2(\theta)}{f_1(\theta)}$
1	−1	$f(\theta)\cos\gamma_k \angle \dfrac{-f_2(\theta)}{f_1(\theta)}$
−1	1	$f(\theta)\cos\gamma_k \angle \dfrac{f_2(\theta)}{-f_1(\theta)}$
−1	−1	$f(\theta)\cos\gamma_k \angle \dfrac{-f_2(\theta)}{-f_1(\theta)}$

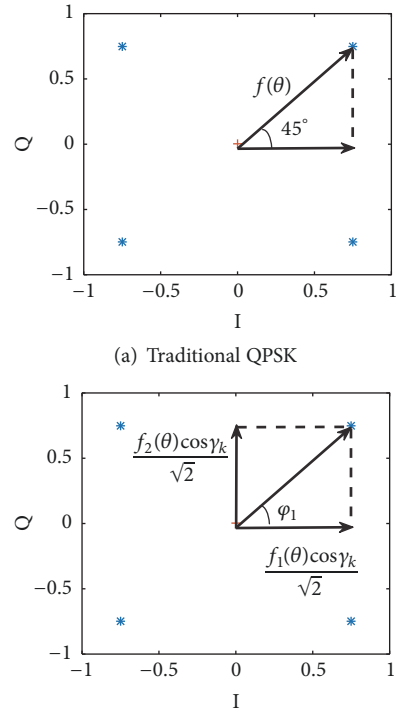

(a) Traditional QPSK

(b) QPSK in polarization 1

Figure 3: QPSKP constellation structure.

Considering the data of polarization 1, it is found that, by changing b_m and c_m, QPSK signals can be obtained as shown in Figure 3 and Table 2 shows the received vectors of the QPSK in polarization 1 (QPSKP) with the b_m and c_m created by the four sets of values ((1,1),(-1,1),(1,-1),(-1,-1)). For QPSKP, the Euclidean distance between the two constellation points is associated with $f_1(\theta)$ and $f_2(\theta)$, unlike the traditional QPSK signal which only depends on $f(\theta)$. In the desired direction, the constellation structure of QPSKP is the same as that of QPSK, while it scrambles when the receiver is off the desired azimuth angle. Thus, the constellation structure received by users in different azimuth angle is changing along with the array gain of dual beams, and this is the key technology for secure transmission, which is similar to the dual-beam directional modulation (DM) technology in [12].

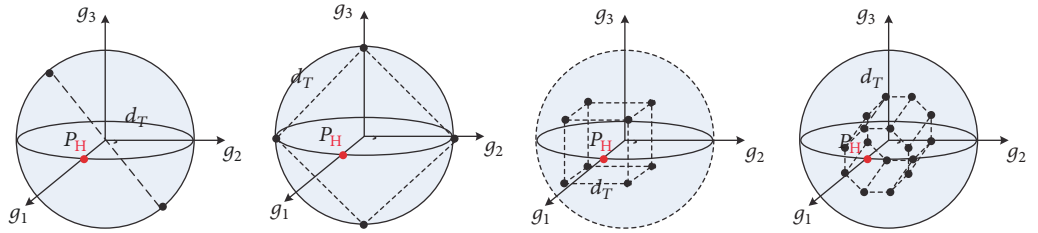

(a) 2PM (b) 4PM (c) 8PM (d) 16PM

FIGURE 4: M_1-th order PM constellation structure [16].

On the other hand, in the desired direction, (6) can be rewritten as

$$\mathbf{y} = \begin{bmatrix} F_1 \\ F_2 \end{bmatrix} = A \begin{bmatrix} f_1(\theta) \cos\gamma_k \cos(w_c t - \varphi_1) + n_1 \\ f_1(\theta) \sin\gamma_k \cos(w_c t + \varphi_2) + n_2 \end{bmatrix}, \quad (8)$$

where $f_1(\theta)=f_2(\theta)$. It is easy to find that the maximum amplitude of F_1 is unaffected by b_m and c_m. Therefore, during every symbol period, the receiver can obtain the polarization parameters by

$$\gamma_k^{\mathrm{R}} = \arctan\left(\mathrm{abs}\left(\frac{\max(|F_2|)}{\max(|F_1|)}\right)\right), \quad \eta_k^{\mathrm{R}} = \Xi(F_2) \quad (9)$$

where $\Xi(\bullet)$ is the phase acquisition operation.

With polarization parameters, PS of the transmitted signal can be gotten and inverse mapping can be conducted to recover the useful information.

Obviously, the transmitted signal's PS is also affected by the array gain of dual beams and only in the desired directions (45°,135°) where $f_1(\theta) = f_2(\theta)$ that $\gamma_k^{\mathrm{R}} = \gamma_k, \eta_k^{\mathrm{R}} = \eta_k$. While in other directions, polarization constellation structure is distorted. In this way, the secure transmission performance is also enhanced by PM. In addition, the combination of M_1-th order PM and M_2-th DM would result in a $(M_1 \times M_2)$-th order modulation scheme, which significantly improves the spectrum efficiency.

4. Performance Evaluation

In this section, security performance is evaluated in terms of symbol error rate (SER) as in [19]. According to the analysis in [11], the SER of DM signals can be calculated by

$$P_{\mathrm{error}} = \sum_{i=1}^{M_2} Q\left(\frac{d_i}{\sqrt{N_0}}\right), \quad (10)$$

where d_i is the smallest Euclidean distance between the i-th constellation point to the other constellation points and M_2 is the modulation order. Thus, for the DM signal in polarization 1 (DMP) during the k-th symbol time, the SER can be calculated as

$$P_{\mathrm{DMP}} = \begin{cases} Q\left(A\cos\gamma_k \sqrt{\dfrac{f_1(\theta)^2 + f_2(\theta)^2}{2N_0}}\right), & M_2 = 2; \\ \dfrac{1}{2}\left(\begin{array}{l} Q\left(A\cos\gamma_k \sqrt{\dfrac{f_1(\theta)^2}{N_0}}\right) \\ +Q\left(A\cos\gamma_k \sqrt{\dfrac{f_2(\theta)^2}{N_0}}\right) \end{array}\right), & M_2 = 4, \end{cases} \quad (11)$$

where N_0 is the noise power spectral density and $Q(\bullet)$ is the complementary Gaussian error function.

For PM, the constellation structure is assumed to be the same as in [16, 18, 21]. The PM constellation structures used in our research are shown in Figure 4. M_1 equipower constellation points with the equal minimum constellation distance d_{T} are placed symmetric to the g_1-axis of the unitary Poincare sphere and each constellation point denotes a unique PS.

As we know, the signal's PS depends on η and γ; therefore, the SER of SEDPM is composed of two parts: the SER from η expressed as P_η and the SER from γ expressed as P_γ. For the parameter η, the SER can be calculated according to (10), which is similar to the calculation in (11). We omit here and denote the SER of η by P_η. In addition, it is noted that, in any directions, the distance between the received constellation points is not affected by changes in η_k^{R} but γ_k^{R} and the received signal to noise ratio (RSNR) [18]. For parameter γ, according to (6) and (9), the received power and the spherical constellation distance between the received adjacent points can be respectively calculated as

$$E_{\mathrm{R}k} = A^2\left(\left(\frac{f(\theta)\cos\gamma_k\cos(w_c t - \varphi_1)}{\sqrt{2}}\right)^2 + \left(\hat{f}(\theta)\sin\gamma_k\cos(w_c t + \varphi_2)\right)^2\right), \quad (12)$$

$$d_{ij}^{\mathrm{R}} = \begin{cases} \arccos\left[\cos^2(2\gamma_i^{\mathrm{R}}) + \sin^2(2\gamma_i^{\mathrm{R}})\cos O\right] & (M = 2, 4) \\ 2\left|\gamma_i^{\mathrm{R}} - \gamma_j^{\mathrm{R}}\right| & (M > 4,\ \gamma_i^{\mathrm{R}} \neq \gamma_j^{\mathrm{R}}) \\ \arccos\left[\cos^2(2\gamma_i^{\mathrm{R}}) + \sin^2(2\gamma_i^{\mathrm{R}})\cos O\right] & (M > 4,\ \gamma_i^{\mathrm{R}} = \gamma_j^{\mathrm{R}}) \end{cases} \quad (13)$$

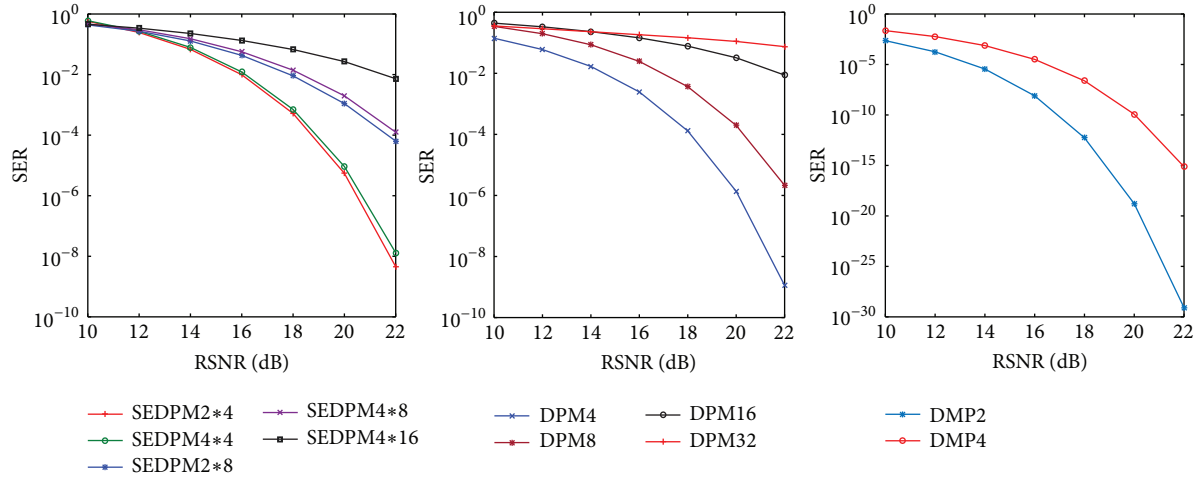

Figure 5: The SER of SEDPM, DPM, and DMP versus RSNR.

where O is the spheric angle between the adjacent polarization constellation points and can be calculated as

$$O = \angle P_i P_H P_j = 2 \arcsin\left[\frac{\sin\left(d_T/2\right)}{\sin\left(2\gamma_i\right)}\right], \tag{14}$$

where d_T is the original spherical constellation distance and P_H is the horizontal PS. Affected by changes in γ_i^R, the spherical distance of the received constellation points becomes small. Then the SER can be calculated as

$$P_\gamma = \frac{1}{M}\sum_{i=1}^{M} SER_i \tag{15}$$

$$SER_i = \sum_{j=1}^{c} 2\left[\begin{array}{l}\displaystyle\int_{\psi_{ij}}^{\pi}\int_{0}^{\alpha(\vartheta_{ij},\psi_{ij})} f\left(t_i,\varphi_i\right)\mathrm{d}\varphi_i\mathrm{d}t_i \\ \displaystyle+\int_{\vartheta_{ij}}^{\psi_{ij}}\int_{0}^{\alpha(\vartheta_{ij},t_i)} f\left(t_i,\varphi_i\right)\mathrm{d}\varphi_i\mathrm{d}t_i\end{array}\right], \tag{16}$$

$$M > 2,$$

where $\alpha(\vartheta_{ij}, t_i) = \arccos(\tan\vartheta_{ij}/t_i)$ and $f(t_i, \varphi_i)$ is the joint probability density function of PS_i's colatitude t_i and azimuth φ_i with additional AWGN noise, which can be expressed as

$$f\left(t_i,\varphi_i\right) = \frac{\sin t_i}{4\pi} e^{-E_{Rk}(1-\cos t_i)/(2N_0)}\left[1+\frac{E_{Rk}\left(1+\cos t_i\right)}{\left(2N_0\right)}\right], \tag{17}$$

where φ_j and t_j are colatitude and azimuth of PS_j and the received signal to noise ratio $RSNR = E_{Rk}/N_0$. $\vartheta_{ij} = d_{ij}^R/2$ denotes the half adjacent constellation spherical distance and ψ_{ij} denotes the sphere distance between PS_i and the endpoints of its decision region (c is the number of endpoints), which can be calculated as

$$\begin{aligned}
&\psi_{i1} = 2\gamma_i^R, \\
&\psi_{i2} = \pi - 2\gamma_i^R, \\
&\qquad\left(M = 4;\ i \in [1,4]\right);\ k = 2 \\
&\psi_{i1} = \psi_{i2} \\
&\quad = \arccos\left[\frac{\cos 2\gamma_i^R + \sin 2\gamma_i^R \tan\left(\gamma_i^R + \gamma_{i+M/2}^R\right)}{1+\sec^2(O/2)\tan^2\left(\gamma_i^R+\gamma_{i+M/2}^R\right)}\right] \\
&\psi_{i3} = 2\gamma_i^R, \quad \left(M \geqslant 8;\ i \in \left[1, \frac{M}{2}\right]\right);\ k = 3 \\
&\psi_{i1} = \psi_{i2} \\
&\quad = \arccos\left[\frac{\cos\left(\gamma_i^R - \gamma_{i-M/2}^R\right)}{1+\sin^2\left(\gamma_i^R+\gamma_{i-M/2}^R\right)\tan^2(O/2)}\right] \\
&\psi_{i3} = \pi - 2\gamma_i^R, \quad \left(M \geqslant 8;\ i \in \left[\frac{M}{2}, M\right]\right);\ k = 3
\end{aligned} \tag{18}$$

For PM, the SER can be calculated by

$$P_{PM} = 1 - \left(1 - P_\eta\right)\left(1 - P_\gamma\right), \tag{19}$$

For SEDPM, the SER can be calculated as

$$P_{SEDPM} = \frac{\left(P_{PM}R_P + P_{DMP}R_D\right)}{\left(R_P + R_D\right)}. \tag{20}$$

where R_P and R_D are the symbol rate realized by the PM and DMP during 1 second.

5. Numerical Results

In our simulations, XPD is assumed to be infinite and the SER of SEDPM is investigated under the additive white Gaussian noise (AWGN) channel. The signal power of the desired direction (45° and 135°) is used as a standard signal power and the overall power of the transmit signal is set to be the same for SEDPM and DPM.

Figure 5 shows the SER of SEDPM, directional modulation in polarization 1 (DMP), and directional polarization

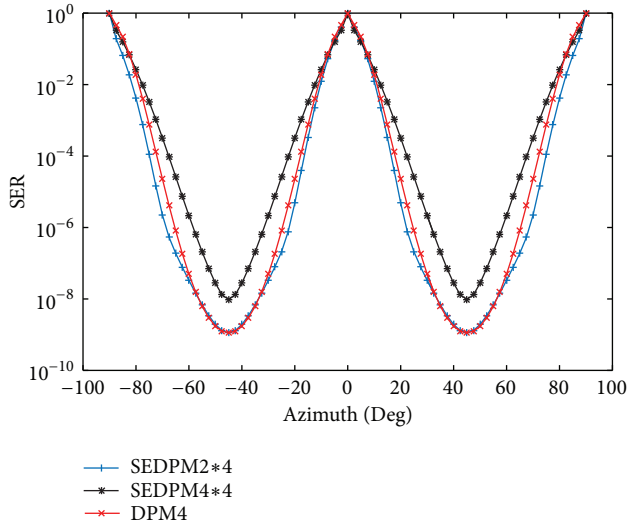

Figure 6: The SER of SEDPM, DPM, and DMP versus azimuth angle.

modulation (DPM) in [12] versus RSNR in the desired direction. The number after DPM and DMP denote the modulation order, and the number after SEDPM represents M_1-th order PM combined with M_2-th order DMP, which results in the $M = M_1 \times M_2$ order SEDPM. For DMP, the SER is excellent and according to (20), it is found that it has little influence on the output SER of SEDPM while improving the spectrum efficiency. Additionally, by comparing SEDPM2∗4 and SEDPM4∗4, it is found that their SER curves achieve almost the same value as DPM4, while the modulation order is higher. In addition, the SER performance of SEDPM4∗4 is better than SEDPM2∗8 and this is because the SER deteriorates quickly as the modulation order grows high for PM. Moreover, for high order modulation, the SEDPM scheme can also achieve a better performance than DPM. Therefore, higher transmission efficiency can be achieved by the SEDPM scheme.

Figure 6 shows the SER versus azimuth angle for DPM4, SEDPM2∗4, and SEDPM4∗4 when RSNR=22dB. It is shown that the SER of SEDPM2∗4 is almost the same as that of DPM4 in the desired directions and deteriorates quickly in other directions, while SEDPM2∗4 has a high modulation order. Moreover, the SER of SEDPM4∗4 is a little worse due to its high modulation order, but its SER deteriorates more quickly out of the main lobe than the other two, which means, in the high modulation order, the performance of the proposed scheme is more outstanding. This characteristic of the proposed scheme is beneficial for the secure wireless communication.

6. Conclusion

In this letter, a spectrum efficient secure transmission scheme based on PM is proposed for the wireless communication system. Both the transmission security and the spectrum efficient can be improved. At last, the performance of the proposed scheme is analyzed and compared with the DPM approach.

Data Availability

The data used to support the findings of this study are available from the corresponding author upon request.

Conflicts of Interest

The authors declare that they have no conflicts of interest.

Acknowledgments

This work is supported by the Equipment Advance Research Fund (no. 6142010020103).

References

[1] W. Roh, J.-Y. Seol, J. Park et al., "Millimeter-wave beamforming as an enabling technology for 5G cellular communications: theoretical feasibility and prototype results," *IEEE Communications Magazine*, vol. 52, no. 2, pp. 106–113, 2014.

[2] P. A. Dzagbletey and Y.-B. Jung, "Stacked Microstrip Linear Array for Millimeter-Wave 5G Baseband Communication," *IEEE Antennas and Wireless Propagation Letters*, 2018.

[3] Z. Luo and H. Wang, "Dual-Polarized Phased Array Based Polarization State Modulation for Physical-Layer Secure Communication," *IEICE Transactions on Fundamentals of Electronics, Communications and Computer Sciences*, vol. E101.A, no. 5, pp. 740–747, 2018.

[4] M. Yofune, J. Webber, K. Yano, H. Ban, and K. Kobayashi, "Optimization of signal design for poly-polarization multiplexing in satellite communications," *IEEE Communications Letters*, vol. 17, no. 11, pp. 2017–2020, 2013.

[5] G. Zafari, M. Koca, and H. Sari, "Spatial modulation with dual-polarized antennas," in *Proceedings of the IEEE International Conference on Communications, ICC 2015*, pp. 2375–2380, UK, June 2015.

[6] D. Wei, M. Zhang, W. Fan, and W. Huang, "A spectrum efficient polarized PSK/QAM scheme in the wireless channel with polarization dependent loss effect," in *Proceedings of the 2015 22nd International Conference on Telecommunications, ICT 2015*, pp. 249–255, Australia, April 2015.

[7] D. Wei, C. Feng, C. Guo, and L. Fangfang, "A power amplifier energy efficient polarization modulation scheme based on the optimal pre-compensation," *IEEE Communications Letters*, vol. 17, no. 3, pp. 513–516, 2013.

[8] Z. Gan, P. Arapoglou, and B. Ottersten, "Physical layer security in multibeam satellite systems," *IEEE Transactions on Wireless Communications*, vol. 11, no. 2, pp. 852–863, 2012.

[9] S. Bayat, R. H. Y. Louie, Z. Han, B. Vucetic, and Y. Li, "Physical-layer security in distributed wireless networks using matching theory," *IEEE Transactions on Information Forensics and Security*, vol. 8, no. 5, pp. 717–732, 2013.

[10] M. P. Daly and J. T. Bernhard, "Beamsteering in pattern reconfigurable arrays using directional modulation," *IEEE Transactions on Antennas and Propagation*, vol. 58, no. 7, pp. 2259–2265, 2010.

[11] M. P. Daly and J. T. Bernhard, "Directional modulation technique for phased arrays," *IEEE Transactions on Antennas and Propagation*, vol. 57, no. 9, pp. 2633–2640, 2009.

[12] T. Hong, M.-Z. Song, and Y. Liu, "Dual-beam directional modulation technique for physical-layer secure communication," *IEEE Antennas and Wireless Propagation Letters*, vol. 10, pp. 1417–1420, 2011.

[13] F. Shu, X. Wu, J. Li, R. Chen, and B. Vucetic, "Robust synthesis scheme for secure multi-beam directional modulation in broadcasting systems," *IEEE Access*, vol. 4, pp. 6614–6623, 2016.

[14] M. Hafez, T. Khattab, T. Elfouly, and H. Arslan, "Secure multiple-users transmission using multi-path directional modulation," in *Proceedings of the 2016 IEEE International Conference on Communications, ICC 2016*, Malaysia, May 2016.

[15] F. Shu, L. Xu, J. Wang, W. Zhu, and X. Zhou, "Artificial-noise-aided secure multicast precoding for directional modulation systems," *IEEE Transactions on Vehicular Technology*, no. 99, 2017.

[16] Z. Luo, H. Wang, K. Zhou, and W. Lv, "Combined Constellation Rotation with Weighted FRFT for Secure Transmission in Polarization Modulation Based Dual-Polarized Satellite Communications," *IEEE Access*, vol. 5, pp. 27061–27073, 2017.

[17] W. Dong, F. Chunyan, and G. Caili, "An optimal precompensation based joint polarization-amplitude-phase modulation scheme for the power amplifier energy efficiency improvement," in *in IEEE International Conference on Communications (ICC, Conference Proceedings*, pp. 4137–4142.

[18] Z. Luo, H. Wang, and W. Lv, "Directional polarization modulation for secure transmission in dual-polarized satellite MIMO systems," in *Proceedings of the 2016 8th International Conference on Wireless Communications & Signal Processing (WCSP)*, pp. 1–5, Yangzhou, China, October 2016.

[19] L. Arend, R. Sperber, M. Marso, and J. Krause, "Implementing polarization shift keying over satellite - system design and measurement results," *International Journal of Satellite Communications and Networking*, vol. 34, no. 2, pp. 211–229, 2016.

[20] H.-B. Song, J.-B. Zhang, X.-G. Chen, and J.-Q. Zhang, "Three-dimensional polarization amplitude modulator and demodulator," *Tongxin Xuebao/Journal on Communication*, vol. 33, no. 9, pp. 15–22, 2012.

[21] W. Dong, F. Chunyan, and G. Caili, "Polarization mode dispersion tolerant subcarrier-power allocation for improving the power amplifier energy efficiency of joint polarization-amplitude-phase modulation," in *Proceedings of the IEEE 77th Vehicular Technology Conference (VTC Spring)*, pp. 1–6, 2013.